JACS
JOURNAL OF THE AMERICAN CHEMICAL SOCIETY
Communication
pubs.acs.org/JACS

Enhanced N_2 Dissociation on Ru-Loaded Inorganic Electride

Navaratnarajah Kuganathan,[†] Hideo Hosono,[‡] Alexander L. Shluger,[†] and Peter V. Sushko*,[†]

[†]Department of Physics and Astronomy and London Centre for Nanotechnology, University College London, Gower Street, London, WC1E 6BT, U.K.

[‡]Frontier Research Center and Materials and Structures Laboratory, Tokyo Institute of Technology, Yokohama 226-8503, Japan

Supporting Information

ABSTRACT: Electrides, i.e. salts in which electrons serve as anions, are promising materials for lowering activation energies of chemical reactions. *Ab initio* simulations are used to investigate the effect of the electron anions in a prototype mayenite-based electride (C12A7:e^-) on the mechanism of N_2 dissociation. It is found that both atomic and molecular nitrogen species chemisorb on the electride surface and become negatively charged due to the electron transfer from the substrate. However, charging alone is not sufficient to promote dissociation of N_2 molecules. In the presence of Ru, N_2 adsorbs with the formation of a *cis*-Ru_2N_2 complex and the N−N bond weakens due to both the electron transfer from the substrate and interaction with Ru. This complex transforms into a more stable *trans*-Ru_2N_2 configuration, in which the N_2 molecule is dissociated, with the calculated barrier of 116 kJ mol^{-1} and the overall energy gain of 72 kJ mol^{-1}. In contrast, in the case of the stoichiometric mayentie, the *cis*-Ru_2N_2 is ∼34 kJ mol^{-1} more stable than the *trans*-Ru_2N_2, while the *cis*−*trans* transition has a barrier of 192 kJ mol^{-1}. Splitting of N_2 is promoted by a combination of the strong electron donating power of C12A7:e^-, ability of Ru to capture N_2, polarization of Ru clusters, and electrostatic interaction of negatively charged N species with the surface cations.

Ammonia is a generic precursor essential for the production of fertilizers, explosives, and other N-containing chemical compounds. It is easily liquefied, making it a convenient high hydrogen-density carrier. Industrial production of NH_3 is carried out using the Haber−Bosch (HB) process, in which dissociation of N_2 is the rate-limiting step.[1,2] Due to the large dissociation energy of N_2 (945 kJ mol^{-1}),[3,4] this process requires pressures of 20−40 MPa and temperatures of ∼400−600 °C. There is great demand for NH_3 synthesis under milder conditions as it would bring energy savings and lessen the technological risks associated with high-pressure processes. Reducing the activation energy for N_2 splitting is a key to achieving this aim. Research in this area focuses on biological,[5−7] solid-state, and surface science,[8−10] synthesis of metal complexes,[11−14] and matrix-isolation gas-phase systems.[15−18]

A recent experimental study demonstrates that the Ru-loaded surface of C12A7 electride acts as an efficient catalyst for NH_3 synthesis at pressures as low as 0.1 MPa and temperatures of 400 °C.[19] Moreover, the measured activation energy for the NH_3 formation is <50 kJ mol^{-1}, which is nearly a half of that reported previously for other Ru-loaded catalysts and an HB catalyst, while the catalytic activity is increased by an order of magnitude.[19] In addition, hydrogen poisoning, a common drawback of Ru catalysts, is noticeably reduced. This clearly indicates that the C12A7 substrate and its unique properties play a significant role in this process. At the same time, it raises questions regarding the mechanism of N_2 dissociation and active sites for N_2 splitting and NH_3 synthesis as a whole. Here, we use *ab initio* modeling (see Supporting Information (SI)) to investigate how the C12A7 characteristic surface structures and electronic properties, together with Ru metal clusters, facilitate the trapping, activation, and splitting of N_2 molecules.

The cubic unit cell of C12A7, also known as mayenite, has the lattice constant of ∼1.2 nm and can be described by the formula $[Ca_{24}Al_{28}O_{64}]^{4+}\cdot 2O^{2-}$, where the cation denotes the framework of 12 equivalent cages, each having an effective charge of +1/3 |e| and the diameter of the inner free space of ∼0.4 nm. The two O^{2-} ions occupy 2 out of 12 cages of the unit cell. These ions diffuse via the interstitialcy mechanism[20] and can be extracted from the lattice leaving behind four electrons per unit cell. The resulting system is described by the formula $[Ca_{24}Al_{28}O_{64}]^{4+}\cdot 4e^-$, where the four electrons localize in the framework cages (1/3 e^- per cage) and are regarded as electronic anions. Hence, this system is called C12A7 electride or, for brevity, C12A7:e^-.[21,22] The framework cages give rise to a narrow partially occupied conduction band (cage conduction band)[23] and an exceptionally low work function of ∼2.4 eV.[24] The surface of C12A7:e^- contains low-coordinated cations associated with the broken framework cages, while the near-surface region retains elements of the bulk structure, such as cages accommodating the anionic electrons.[25,26] We demonstrate that these features, together with the low value of the C12A7:e^- work function and enhanced polarizability of Ru clusters, facilitate the splitting of N_2.

Figure 1 shows adsorption energies of N atoms and N_2 molecules on the pure and Ru-containing surfaces of stoichiometric and electride C12A7 and the total charge associated with each Ru_xN_y species. In the case of the C12A7:O^{2-} surface, N_2 molecules physisorb with binding energies <10 kJ mol^{-1}. In contrast, N atoms adsorb with binding energies of 10−40 kJ mol^{-1}, depending on the surface site, and acquire the charge in the range from −0.1 to −0.7 |e|, which is transferred from the low-coordinated surface O^{2-} ions.

In the case of C12A7:e^-, the near-surface cages contain two electrons,[26] which can be readily trapped by the adsorbed species. In particular, N_2 molecules chemisorb with binding energies of

Received: October 25, 2013
Published: January 20, 2014

   dx.doi.org/10.1021/ja410925g | J. Am. Chem. Soc. 2014, 136, 2216−2219

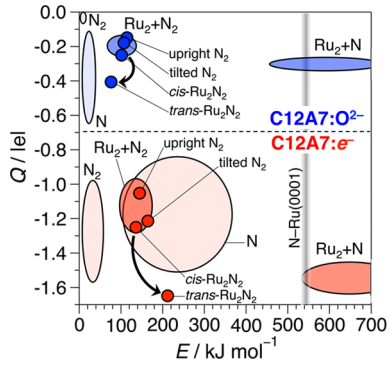

Figure 1. Adsorption energies (E) for N atoms and N_2 molecules on the pure and Ru-containing stoichiometric (top, blue) and electride (bottom, red) C12A7 surfaces. Q indicates the total charges of the Ru_xN_y complexes. Light- and dark-shaded areas correspond to the pure and Ru-containing C12A7, respectively. Characteristics of four configurations (see geometrical structures in Figures 2 and S2) are shown explicitly. Arrows correspond to the N_2 dissociation pathways for a Ru_2N_2 complex on C12A7:O^{2-} and C12A7:e^-. Adsorption energy of N atoms on Ru(0001) surface is shown for comparison.

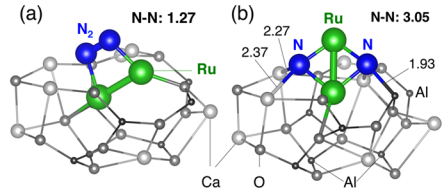

Figure 2. Geometrical configurations of the *cis*-Ru_2N_2 (a) and *trans*-Ru_2N_2 (b) complexes at the broken cage site, shown in gray scale. Spheres show (in the order of increasing radii): Al (black), O (dark gray), Ca (light gray), N (blue), Ru (green). Numbers indicate the interatomic distances in Å.

up to 50 kJ mol^{-1}; the charge of the molecules after adsorption varies between −1.0 and −1.6 |e|. As a result, the N−N bonds elongate by up to ∼0.13 Å, and the calculated N_2 stretching frequencies decrease to 1460−1830 cm^{-1}, i.e., become significantly lower than that of the gas phase N_2 molecule (2433 cm^{-1}). The adsorption energies for N atoms are between 116 and 357 kJ mol^{-1}, and the charge transferred from the C12A7:e^- substrate to these atoms varies between −0.8 and −1.5 |e|. The Ca−N bonds, formed in this case, have the bond lengths of 2.16−2.54 Å, which is comparable to the Ca−N distance in Ca_3N_2 (2.45 Å).

Electron-rich surface defects, such as H^+/e^- centers[27,28] and atoms of alkali metals[29] on insulating surfaces, can increase the binding energy of N_2 with respect to that on nondefective surfaces. Here we investigate the effect of Ru deposited on C12A7:O^{2-} and C12A7:e^- surfaces (see SI). Ru atoms adsorb on C12A7:O^{2-} with the energy gain of 190−290 kJ mol^{-1} and form covalent bonds with low-coordinated O atoms, as manifested by negligible amount of charge transferred between the surface and the adsorbed Ru. In the case of the C12A7:e^- surface, the range of Ru atom binding energies is 390−480 kJ mol^{-1} and as much as −1.25 |e| is transferred from the C12A7:e^- surface to the adsorbed Ru atom.

Ru dimers (Ru_2) also strongly bind to both stoichiometric and electride surfaces. These dimers are neutral on the C12A7:O^{2-} surface. In contrast, on the C12A7:e^- surface, approximately −1.50 |e| is transferred from the near-surface cages to Ru. Since the experimentally observed work function of C12A7:e^- is 2.4 eV (232 kJ mol^{-1}) and that of the bulk Ru metal is 4.7 eV (453 kJ mol^{-1}), the surface-to-Ru charge transfer is expected to take place in the case of larger Ru clusters and nanoparticles (NPs) as well.[19] The charge distribution in the adsorbed Ru clusters is affected by their local atomic environment. For example, in some of the most stable configurations of the Ru_2 cluster, the Ru atomic charges are −0.50 |e| and +0.28 |e| on C12A7:O^{2-} and −0.94 |e| and −0.45 |e| on C12A7:e^- surfaces. Such polarization of Ru affects the charge distribution in the adsorbed N species as discussed below.

Adsorption energies of N atoms and N_2 molecules calculated for the Ru-containing surfaces are larger than those found for pure C12A7 (Figure 1). Similarly to the case of the pure surfaces, the binding is stronger for C12A7:e^- than for C12A7:O^{2-} and the Ru_xN_y moieties are more negatively charged on C12A7:e^- than on C12A7:O^{2-}.

In the following we focus on the interaction of N_2 molecules and the Ru-loaded C12A7:e^- surface. We found that N_2 binds most strongly to the Ru_2 cluster occupying the center of a broken cage on the C12A7:e^- surface (see Figure 2). The cage center is a natural anion site in the bulk C12A7 lattice. Similarly, the broken cage site for the surface is a natural binding site of negatively charged adsorbed species.

Figure 1 shows the binding energies of N_2 to the Ru_2 cluster at this site for four configurations corresponding to various stages of the adsorption process. First, we considered N_2 oriented perpendicularly to the plane of the surface and binding to the Ru_2 cluster. The corresponding geometrical structure is shown in Figure S2. This configuration, denoted as upright N_2 in Figure 1, is metastable; it relaxes to the tilted N_2 configuration with an energy gain of ∼27 kJ mol^{-1} (Figure 1). Interestingly, the N_2 bond length in the tilted configuration is only 1.19 Å, which suggests that the intramolecular bonding remains largely unaffected by the adsorption process.

The tilted N_2 configuration can transform into a *cis*-type complex (Figure 2a), formed by N_2 binding laterally to the Ru_2 cluster, with the calculated barrier of 30 kJ mol^{-1} (see also Figure S4 in SI). The overall N_2 adsorption energy is 144 kJ mol^{-1}, and the resulting N−N bond length is 1.27 Å. Despite such a large elongation of the N−N bond, this configuration is only 20 kJ mol^{-1} less stable than the tilted N_2 configuration. We attribute this effect primarily to two factors. First, the larger N−N distance corresponds to the smaller splitting between the highest occupied and the lowest unoccupied states of the molecule, which facilitates electron transfer (ET) from Ru_2 to N_2 and, thus, makes the stretching of the N−N bond less energy demanding. In addition, the stability of the *cis*-Ru_2N_2 complex is helped by the formation of the second Ru−N bond. We note that, in the case of the larger Ru clusters (see SI), the range of adsorption energies for the monodentate N_2 overlaps with that of the bidentate N_2 configurations. However, the N−N interatomic distances in the former are below 1.19 Å, which suggests that they are unlikely to be precursor states for the N_2 dissociation process.

The configuration shown in Figure 2b is a bis-nitrido species Ru(μ-N)$_2$Ru; for simplicity we call it *trans*-Ru_2N_2. On C12A7:e^-, the *trans*-Ru_2N_2 complex is 72 kJ mol^{-1} more stable than the *cis*-Ru_2N_2 and the most stable one among all considered configurations of Ru_2N_2. In this case, the distance between the two N atoms exceeds 3 Å; i.e., the N−N bond is cleaved.

Similar configurations were found for the Ru_2 at the C12A7:O^{2-} surface (see Figure 1). In this case, the N_2 adsorption energy in the *cis*-Ru_2N_2 configurations is 106 kJ mol^{-1}, and importantly, the dissociated N_2 configuration (*trans*-Ru_2N_2) is 34

dx.doi.org/10.1021/ja410925g | J. Am. Chem. Soc. 2014, 136, 2216−2219

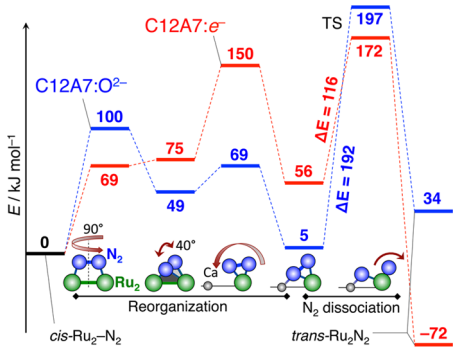

Figure 3. Potential energy diagram for the *cis*–*trans* transformation of the Ru_2N_2 complex on the stoichiometric (blue) and electride (red) C12A7 surfaces and schematics of the corresponding geometrical configurations.

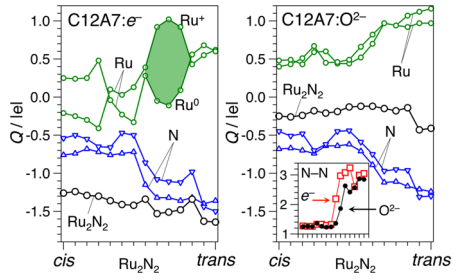

Figure 4. Atomic charges for N and Ru atoms and for Ru_2N_2 complexes along the *cis*-Ru_2N_2–*trans*-Ru_2N_2 transformation path. Inset shows the N–N distances (in Å) along the path for both C12A7:e^- and C12A7:O^{2-} surfaces. The shaded area highlights the part of the path involving polarization of the Ru_2 cluster.

kJ mol^{-1} less stable than the *cis*-Ru_2N_2. We note that the formation of the *cis*-Ru_2N_2 configuration at the Ru-loaded C12A7 surface occurs spontaneously, while the formation of the *trans*-Ru_2N_2 does not.

The potential energy diagram for the *cis*–*trans* transition of the Ru_2N_2 complex on the C12A7:e^- surface is shown in Figure 3, and several intermediate configurations for this transition path are shown in the SI. The path consists of two parts: reorganization of the Ru_2N_2 complex and N_2 dissociation. The first part involves rotation of the N_2 molecule by 90° so that the N–N and Ru–Ru bonds are nearly perpendicular to each other, followed by the rotation of N_2 around the Ru–Ru axis so that one of the N atoms binds to a surface Ca^{2+} ion. The N–Ca distance in this configuration is 2.35 Å, which is similar to that in the bulk Ca_3N_2. In this process, the N_2 molecule preserves its structure (N–N distance is ∼1.25 Å) and the charges of the N_2 and Ru_2 moieties remain unchanged: −1 |e| and ∼0 |e|, respectively, for C12A7:e^- and −1 |e| and +1 |e|, respectively, for C12A7:O^{2-} (Figure 4).

The second part of the path, N_2 dissociation, involves elongation of the N–N bond to 2.2 Å in the transition state (see inset in Figure 4). In the case of the C12A7:e^- surface this corresponds to the potential energy barrier of 116 kJ mol^{-1}. In this configuration, one electron is transferred from Ru_2 to N_2, converting them to Ru_2^+ and N_2^{2-}, respectively (Figure 4). Thus, Ru serves not only as a strong binding site for N_2 but also as an electron donor. We note that the dissociation process is facilitated by polarization of the Ru_2 cluster. As shown with the shaded area in Figure 4, one of the Ru atoms becomes neutral, while the other one becomes more positive (Ru^0 and Ru^+, respectively, in Figure 4). Such disproportionation of the Ru atomic charges induces disproportionation of the N atomic charges, which weakens the N–N bond further. In particular, the N atom located closer to Ru^+ becomes more negatively charged and, therefore, interacts stronger with the cations of the C12A7:e^- surface and binds to the surface Ca^{2+} ions, as schematically shown in Figure 3. At this stage, this nitrogen becomes an ionic species and the dissociation of the covalent N–N bond is effectively completed. This conclusion is supported by the sharp increase of the N–N interatomic distance (see inset in Figure 4). We also note that the Ru_2 cluster becomes more positive along the *cis*–*trans* transformation path, while the Ru_2N_2 complex, as a whole, becomes more negative (Figure 4). This demonstrates that N_2 dissociation and stabilization of the isolated nitrogen ions are assisted by the ET from both the Ru_2 cluster and the C12A7:e^- substrate. We note that the *trans*-Ru_2N_2 configuration, in which N_2 is dissociated, is 72 kJ mol^{-1} more stable than the *cis*-Ru_2N_2 configuration. For comparison, the N_2 dissociation reaction on C12A7:e^- in the absence of Ru is endothermic by ∼300 kJ mol^{-1}.

In the case of the fully oxidized C12A7:O^{2-} surface, the *cis*–*trans* transformation of the Ru_2N_2 complex follows a pathway similar to that found for C12A7:e^-. However, since the Ru atoms are positively charged, the polarization of the Ru cluster is negligible (see Figure 4). This translates into negligible disproportionation of charge within the N_2 molecule and, consequently, makes stabilization of one of the nitrogen species in an ionic configuration less energetically favorable than that in the case of the C12A7:e^- surface. Therefore, the barrier for the N_2 dissociation is 192 kJ mol^{-1} (Figure 3), i.e., significantly higher than in the case of C12A7:e^-.

This demonstrates that the ET from the electride surface is essential to promote N_2 dissociation. Such ET not only weakens the N–N bond due to the positive electron affinity of the N_2 molecule but also enhances polarizability of the Ru and nitrogen species. The latter, in turn, promotes disproportionate charge distribution within N_2 and leads to stabilization of one of the N atoms in the ionic configurations, thus, effectively, breaking the N–N bond. We note that the lowering of the N_2 dissociation barrier due to the electrostatic interaction between the positively charged ions and negatively charged N_2^- has been observed earlier. For example, Na and Cs deposition on the Ru (0001) surface was shown to lower this barrier by ∼14 and ∼30 kJ mol^{-1}, respectively.[30] For comparison, the C12A7:e^- surface provides a much higher concentration of the extra electrons and has a high surface density of Ca^{2+} and Al^{3+} ions. Both of these factors contribute to the electrostatic interaction and, consequently, lower the N_2 dissociation barrier by over 75 kJ mol^{-1}.

Finally, we considered several Ru_n clusters (up to n = 6) on both C12A7:e^- and C12A7:O^{2-} surfaces. In all cases the most energetically stable configurations correspond to the "flat" single atomic layer clusters. This is consistent with the relatively low cohesive energies (250–500 kJ mol^{-1}) found for clusters containing between 3 and 64 Ru atoms.[31] In addition, this suggests that, even though the Ru bulk cohesive energy (∼650 kJ mol^{-1}) is larger than the Ru binding energies to the C12A7 surfaces (see SI), the periphery of the Ru NPs is likely to be dominated by the single Ru layer motifs. Furthermore, it has been noticed that, as the size of a supported metal cluster increases, the effect of its charging on the adsorption energies of molecules decreases.[32,33] This can be explained by the localization of the excess charge on the metal atoms close to the interface. For example, the studies of Pd deposited near a neutral

dx.doi.org/10.1021/ja410925g | J. Am. Chem. Soc. 2014, 136, 2216–2219

oxygen vacancy on MgO(001) show that the electron charge transferred from the substrate to the metal tends to localize close to the vacancy site.[34] This suggests that, in the case of the Ru-loaded C12A7:e^- surface, the electron charge transferred to Ru NPs is localized in the Ru/C12A7 interface region. Only the perimeter of this interface region, i.e., the fringes of the NPs are accessible to the N_2 molecules. This gives support to the Ru_2 cluster model used in this study.

We also note that N atoms formed upon dissociation of N_2 adsorb next to the Ru_2 cluster. The combination of the charge trapping, interaction with the surface Ca^{2+} and Al^{3+} ions, and polarization of Ru_2 results in the adsorption energies of 540−720 kJ mol^{-1} (Figure 1). These can be compared with, for example, adsorption energies of N atoms on various Ru surfaces, most of which are found to be <580 kJ mol^{-1} (see ref 35 and references therein). In other words, N atoms are more likely to stabilize at the interface between Ru NPs and the surface than elsewhere on the NPs. Thus, we propose that the sites forming such interfaces, i.e., the fringes of the Ru NPs deposited on C12A7:e^-, serve as the most active N_2 splitting sites.

To summarize, the charge transfer from the C12A7:e^- surface to the adsorbed N_2 is sufficient to weaken the N−N bond but it does not lead to its dissociation. N_2 adsorption on Ru-loaded C12A7:e^- is stronger than that on the pure C12A7:e^- surface. A single Ru atom is not sufficient to dissociate an N_2 molecule. However, Ru_2 clusters are large enough to facilitate the N_2 dissociations reaction which is exothermic on C12A7:e^- and proceeds with the barrier of 116 kJ mol^{-1}. A similar N_2 dissociation pathway on C12A7:O^{2-} has the barrier of 192 kJ mol^{-1}, and the overall reaction is endothermic. This dramatic difference between the calculated reaction barriers is consistent with the experimental findings;[19] it arises solely from the difference between the properties of the electride C12A7:e^- and stoichiometric C12A7:O^{2-} surfaces. In particular, nitrogen species are stabilized on C12A7:e^- primarily due to the ET from the surface. This charge transfer, aided by the formation of the ionic bonds between the negatively charged nitrogen and surface cations and by the polarization of the Ru cluster, stabilizes the nitrogen species in the ionic electronic configuration and, thus, promotes dissociation of the N_2 molecules.

■ ASSOCIATED CONTENT

Supporting Information

Details of computational procedure; table showing adsorption energies, Bader charges, N−N interatomic distances and N_2 stretching frequencies for the configurations considered in this study; figures showing geometrical configurations of the adsorbed species and N_2 dissociation pathways. This material is available free of charge via the Internet at http://pubs.acs.org.

■ AUTHOR INFORMATION

Corresponding Author

p.sushko@ucl.ac.uk

Notes

The authors declare no competing financial interest.

■ ACKNOWLEDGMENTS

This study was supported by the Funding Program for World-Leading Innovative R&D on Science and Technology (FIRST), Japan Society for the Promotion of Science and the Accelerated Innovation Research Initiative (ACCEL), Japan Science and Technology Agency (JST). P.V.S. is supported by the Royal Society. Calculations have been performed at the HECTOR facility (access provided via the Materials Chemistry Consortium, EPSRC Grant EP/F067496).

■ REFERENCES

(1) Mittasch, A.; Frankenburg, W. *Advances in Catalysis*; Academic Press: San Diego, CA, 1950.
(2) Honkala, K.; Hellman, A.; Remediakis, I. N.; Logadottir, A.; Carlsson, A.; Dahl, S.; Christensen, C. H.; Nørskov, J. K. *Science* **2005**, *307*, 555.
(3) Gambarotta, S.; Scott, J. *Angew. Chem., Int. Ed.* **2004**, *43*, 5298.
(4) Pool, J. A.; Lobkovsky, E.; Chirik, P. J. *Nature* **2004**, *427*, 527.
(5) Burgess, B. K. *Chem. Rev.* **1990**, *90*, 1377.
(6) Burgess, B. K.; Lowe, D. J. *Chem. Rev* **1996**, *96*, 2983.
(7) Rod, T. H.; Nørskov, J. K. *Surf. Sci.* **2002**, *500*, 678.
(8) Ertl, G. *Angew. Chem., Int. Ed. Engl.* **1990**, *29*, 1219.
(9) Ertl, G. *Angew. Chem., Int. Ed.* **2008**, *47*, 3524.
(10) Rao, C. N. R.; Rao, G. R. *Surf. Sci. Rep.* **1991**, *13*, 221.
(11) Kozak, C. M.; Mountford, P. *Angew. Chem., Int. Ed.* **2004**, *43*, 1186.
(12) Fryzuk, M. D. *Chem. Rec.* **2003**, *3*, 2.
(13) Fryzuk, M. D.; Johnson, S. A. *Coord. Chem. Rev.* **2000**, *200−202*, 379.
(14) Shima, T.; Hu, S. W.; Luo, G.; Kang, X. H.; Luo, Y.; Hou, Z. M. *Science* **2013**, *340*, 1549.
(15) Himmel, H. J.; Hubner, O.; Klopper, W.; Manceron, L. *Angew. Chem., Int. Ed.* **2006**, *45*, 2799.
(16) Himmel, H.-J.; Reiher, M. *Angew. Chem., Int. Ed.* **2006**, *45*, 6264.
(17) Kuganathan, N.; Green, J. C.; Himmel, H.-J. *New J. Chem.* **2006**, *30*, 1253.
(18) Himmel, H. J.; Hubner, O.; Bischoff, F. A.; Klopper, W.; Manceron, L. *Phys. Chem. Chem. Phys.* **2006**, *8*, 2000.
(19) Kitano, M.; Inoue, Y.; Yamazaki, Y.; Hayashi, F.; Kanbara, S.; Matsuishi, S.; Yokoyama, T.; Kim, S.-W.; Hara, M.; Hosono, H. *Nat. Chem.* **2012**, *4*, 934.
(20) Sushko, P. V.; Shluger, A. L.; Hayashi, K.; Hirano, M.; Hosono, H. *Phys. Rev. B* **2006**, *73*, 014101.
(21) Matsuishi, S.; Toda, Y.; Miyakawa, M.; Hayashi, K.; Kamiya, T.; Hirano, M.; Tanaka, I.; Hosono, H. *Science* **2003**, *301*, 626.
(22) Kim, S. W.; Matsuishi, S.; Nomura, T.; Kubota, Y.; Takata, M.; Hayashi, K.; Kamiya, T.; Hirano, M.; Hosono, H. *Nano Lett.* **2007**, *7*, 1138.
(23) Sushko, P. V.; Shluger, A. L.; Hirano, M.; Hosono, H. *J. Am. Chem. Soc.* **2007**, *129*, 942.
(24) Toda, Y.; Yanagi, H.; Ikenaga, E.; Kim, J. J.; Kobata, M.; Ueda, S.; Kamiya, T.; Hirano, M.; Kobayashi, K.; Hosono, H. *Adv. Mater.* **2007**, *19*, 3564.
(25) Toda, Y.; Kubota, Y.; Hirano, M.; Hirayama, H.; Hosono, H. *ACS Nano* **2011**, *5*, 1907.
(26) Sushko, P. V.; Shluger, A. L.; Toda, Y.; Hirano, M.; Hosono, H. *Proc. Royal Soc. A* **2011**, *467*, 2066.
(27) Ricci, D.; Pacchioni, G.; Sushko, P. V.; Shluger, A. L. *Surf. Sci.* **2003**, *542*, 293.
(28) Chiesa, M.; Paganini, M. C.; Giamello, E.; Murphy, D. M.; Di Valentin, C.; Pacchioni, G. *Acc. Chem. Res.* **2006**, *39*, 861.
(29) Edwards, P. P.; Anderson, P. A.; Thomas, J. M. *Acc. Chem. Res.* **1996**, *29*, 23.
(30) Mortensen, J. J.; Hammer, B.; Nørskov, J. K. *Phys. Rev. Lett.* **1998**, *80*, 4333.
(31) Zhang, W.; Zhao, H.; Wang, L. *J. Phys. Chem B* **2004**, *108*, 2140.
(32) Lopez, N.; Janssens, T. V. W.; Clausen, B. S.; Xu, Y.; Mavrikakis, M.; Bligaard, T.; Norskov, J. K. *J. Catal.* **2004**, *223*, 232.
(33) Mills, G.; Gordon, M. S.; Metiu, H. *J. Chem. Phys.* **2003**, *118*, 4198.
(34) Giordano, L.; Goniakowski, J.; Pacchioni, G. *Phys. Rev. B* **2003**, *67*, 045410-1.
(35) Liu, S. P.; Hao, C.; Li, S. M.; Wang, Z. X. *Appl. Surf. Sci.* **2009**, *255*, 4232.